THE INNER SURFACE TRACTION OF CURVED DIES FOR EXTRUSION AND DRAWING OF SOLID RODS USING FI/SSM +

Dr. Kamal Mustafa Kamal Saify *

Abstract:

A successful attempt, to evaluate the internal pressure and shear stresses on the direct extrusion-die surface of arbitrary profile, is presented in this paper, adopting the modified sheared-slab method (SSM), recently developed, which accounts for the transverse shear effect, not included in the classical slab method (CSM). The method employs a finite-integral procedure (FI) for solving of the governing differential equations of stress-equilibrium and applies a convergence pattern test for results check. Two typical profiles of the die surface generators (the truncated conical and radial convex ones) were selected to run the procedure. The entire geometrical and mechanical properties, effecting on the surface traction level values, were maintained in (those like: area reduction, artificial die-angle and friction factor). The problem of finite-element stress analysis and mechanical behavior of the complete die-region, for safety design purpose, can be now achieved reliably as soon as the die internal loading is properly estimated, a matter which this treatise offers to.

المستخلص:

محاولة ناجحة لتحديد الضغط السطحي الداخلي والقص الاحتكاكي على قالب بثق مباشر ذو شكل هندسي إعتباطي، قد تم تقديمها في هذه الورقة، معتمدةً على طريقة اللوحة القصية المطورة (SSM) والمشتقة حديثاً والتي تأخذ في الحساب تأثير القص المستعرض لأول مرة (المهمل في طريقة اللوحة الكلاسيكية (CSM)). وظفت الطريقة الجديدة أسلوب التكامل المحدد(FI) على المعادلات الحاكمة الجديدة لاتزان الاجهادات مع تطبيق إختبار نموذج التقارب لغرض الوثوق من النتائج. تم إعتماد شكلين هندسيين صناعيين لسطح القالب (المخروط الناقص والمحدب القطري) لاغراض الحسابات العددية مع أخذ تأثير كل المتغيرات الهندسية والميكانيكية. إن مسألة تحليل الاجهاد والتصرف الميكانيكي بطريقة العناصر المحددة (FEM) لمادة القالب، تصبح الآن متيسرة التطبيق لتوفر عنصر الحمل الخارجي (External loading)، الأمر الذي تبنته الورقة الحالية كهدف أساسي.

Notations:

k	Yield shear stress.	α	Die semi-angle.
L	Die length.	β	Billet radius ratio.
m	Friction factor.	φ	Tangent of α.
N	No. of Die offsets (subdivisions).	γ	Die length to radius ratio.
P_r	Die internal surface pressure.	σ_x	Billet forming stress (x-

+ Received on 1/4/2009 , Accepted on 5/4/2009 .

* Asst. Prof./ Technical College-Baghdad

			direction).
r	Area reduction.	σ_Y	Billet yield stress.
r_0	Die radial profile size.	τ_f	Billet-die frictional stress (shear).
x	Die longitudinal central axis.	τ_s	Billet transverse shear stress.

Introduction :

Extrusion operations had attended superior developments since the first beginning, one century ago. Recently, the huge progress in industrial metal forming processes, surpasses the academic achievements both in theory and analysis which still comprise some lacks in some typical cases[1]. Nowadays, these lacks are overcome empirically by "*trial and error*" technique using so professional automotive machines[2]. The design of the die requires confidential knowledge of the enormous stresses imposed from the ingot plastic deformation and transferred intern to the die bearing area which ought to withstand the big reaction elastically. In cold direct extrusion and drawing processes, the die inner surface represents the border region between the ingot world of plasticity and the die world of elasticity. The localized traction, at this border, is the main quest for satisfactory design of the die and also for correct analysis of the mechanical behavior of the bearing area. For axisymmetric forming process, the point-wise traction composes of two main stresses, the friction shear stress tangent to the die internal surface and the direct compressive stress normal to this surface. The first component is relatively small in magnitude and often modeled constant as long as the billet yield shear stress and the friction factor are assumed unchanged[3]. The second component is much vast in magnitude. It exceeds several levels of the billet yield stress depending on the desired reduction of area and the geometry of the die inner profile. At present, the quantitative evaluating of this component (the die internal pressure) is alternating between the weakened theoretical values by the classical slab method (CSM)[4,5] and the complicated numerical estimations by the finite element method[6,7]. The powerful technique of upper-bound approach (UBA), based upon *Von-Mises* criterions of failure and strain rate constitutive relationships[8,9] for variety suggestions of the velocity discontinuity fields[10,11], is limited to predict the overall thrust of the machine ram and very rarely used to estimate the traction variation on the die. Good agreements had been achieved by these approaches compared with guaranteed results of drawing and extrusion experiments[12]. At moderate and large angles of the conical die, the CSM under-estimates the results very badly, although it gave a full mathematical expression of the die internal pressure. In his paper[13], the present author improved the classical method by introducing the ignored transverse shear stress in the equilibrium equations. The new sheared slab method (SSM), by this manner, seemed to be a real competitor to the confidential UBA, not only due to the acceptable results it assures, rather than the successful expressions of stress derivative functions it supplies. The present work starts indeed from this particular point to solve the axial and normal stress derivative functions from the SSM for arbitrary die inner profile of surface of revolution making use of a simple finite-integral treatment within the physical domain of the ingot plastic deformation from the die entrance to exit positions. For sake of simplicity, the die internal shape is chosen to be industrially tapered (truncated cone) or radially convex. Other artificial curves of the die profile (like radially concave, sine and cosine curves or even numerically hypothetical ones) can be treated similarly.

The direct and shear forming stresses:

Fig.(1,a) shows a schematic drawing of longitudinal half section of a die-billet region for direct extrusion process. The internal die profile is of arbitrary shape of surface of revolution about the central axis *x*, as illustrated in Fig.(1,b). *R* is the radius of selected cross section of the billet. Therefore the die profile would be designated by $R=f(x)$. The main traction, acting upon this profile, due to the billet internal loading, are the internal pressure P_r normal to the curve and the frictional stress τ_f tangent to the same curve. In accordance to the theoretical work made by [13], where the important effect of the billet transverse shear τ_s was included (not shown in the figure), the modified differential equation of the longitudinal forming stress σ_x and the die pressure P_r, were derived as:

$$d\left(\frac{\sigma_x}{\sigma_Y}\right)=\left\{1+\frac{m}{\sqrt{3}}\left(\cot\alpha+\tan\alpha\right)\right\}\frac{2dR}{R}+\tan\alpha.\frac{1}{R^2}.d\left(\frac{\tau_s.R^2}{\sigma_Y}\right)$$

$$P_r=\sigma_Y+\sigma_x+\tan\alpha.\tau_f+\tan\alpha.\frac{1}{2R}\frac{d}{dR}\left(\tau_s.R^2\right) \qquad ......(1-2)$$

The last element, in each of above equations, represents the new extensions upon the classical formulations of the stresses. The notations σ_Y and *m* denote the billet direct flow stress and the billet friction factor (0<m<1) respectively. The mathematical expressions of τ_f and τ_s had been displayed as:

$$\tau_f=m.k \quad , \quad m=\frac{\sigma_Y}{\sqrt{3}}$$

$$\tau_s=\frac{2}{3}k\left(\frac{R-R_{exit}}{R_{ent.}-R_{exit}}\right) \qquad ......(3-5)$$

where *k* refers to the shear yield stress (evaluated here according to *Von-Mices* failure criteria), $R_{ent.}$ and R_{exit} are the internal radii of the die region at entrance and exit locations respectively. Keeping in mind that the present objective is devoted to estimate the internal traction P_r and τ_f when $R=f(x)$, σ_Y and *m* are all being known, then the current problem would be obviously started with solving of eq.(1) for (σ_x/σ_Y) and then using the result for evaluating P_r in eq.(2), whereas eq.(3) implying a constant value of τ_f. The differential eq.(1) can be solved normally by the finite difference technique. However, a finite-integral (FI) procedure[14] would be more convenient, since it performs an "*exact*" solution for truncated conical profiles of the internal die surface. To do so, the die central axis is subdivided into distinct offsets of total number *N* giving

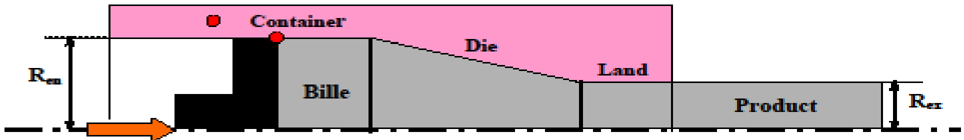

Fig.(1a) Schematic plotting of typical "*truncated conical*" die (with land) for production of solid rod.

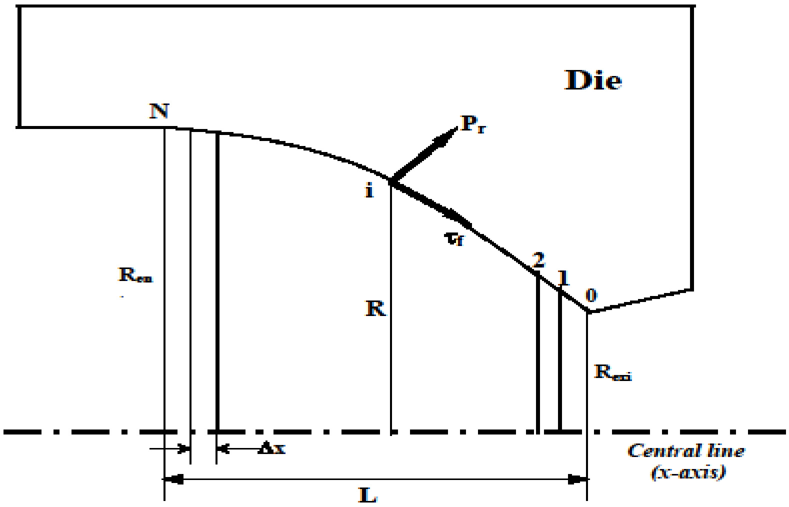

Fig.(1b). A typical die (with out land) of general curved profile (R=f(x)) with usual notations.

an equal interval of $\Delta x=L/N$ between two adjacent offsets. The numbering of these offsets $i=0,1,2,\ldots,N$ begins from die exit $(i=0,\ R=R_0)$ and ending at the die entrance $(i=N,\ R=R_N)$ as shown in the same figure. At each offset i, the associated radius, stresses and profile slope angle would be referred to R_i, σ_{xi}, P_{ri} and α_i respectively. The integrating of eq.(1) in the finite interval Δx from i to i-1 yields to:

$$\left(\frac{\sigma_x}{\sigma_Y}\right)_i-\left(\frac{\sigma_x}{\sigma_Y}\right)_{i-1}=\left\{1+\frac{m}{\sqrt{3}}\left(\cot\alpha_i+\cot\alpha_i\right)\right\}\left(2\ln\frac{R_i}{R_{i-1}}\right)+\frac{2\tan\alpha_i}{3\sqrt{3}}\cdot\left(3\frac{R_i-R_{i-1}}{R_N-R_0}-2\frac{R_0}{R_N-R_0}\ln\frac{R_i}{R_{i-1}}\right)\qquad\ldots\ldots(6)$$

for $i=1,2,\ldots\ldots,N.$

where the slope angle is kept unchanged within particular interval Δx, but not necessary to be of same magnitude for another interval. Introducing the non-dimensional notations of:

$$\beta_i = \frac{R_i}{R_N} \quad , \quad \gamma = \frac{L}{R_N} \quad \text{and} \quad \phi_i = \tan\alpha_i \approx \frac{\beta_i - \beta_{i-1}}{(\gamma / N)} \qquad ......(7\text{-}9)$$

The expression in eqs.(6,2 & 3) shall be altered there to:

$$\left(\frac{\sigma_x}{\sigma_Y}\right)_i = \left(\frac{\sigma_x}{\sigma_Y}\right)_{i-1} + \left\{1 + \frac{m}{\sqrt{3}}(\phi_i + \phi_{i-1}^{-1})\right\}\left(2\ln\frac{\beta_i}{\beta_{i-1}}\right) + \frac{2\phi_i}{3\sqrt{3}}\left(\frac{\beta_i - \beta_{i-1}}{1-\beta_0}\right).$$
$$\left(3 - 2\frac{\beta_0}{\beta_i - \beta_{i-1}}\ln\frac{\beta_i}{\beta_{i-1}}\right)$$

$$\left(\frac{P_r}{\sigma_Y}\right)_i = 1 + \left(\frac{\sigma_x}{\sigma_Y}\right)_i + \frac{m.\phi_i}{\sqrt{3}} + \frac{\phi_i \beta_i}{3\sqrt{3}(1-\beta_0)}\left(3 - 2\frac{\beta_0}{\beta_i}\right)$$

$$\left(\frac{\tau_f}{\sigma_Y}\right)_i = \frac{m}{\sqrt{3}} \qquad \text{for } i = 1,2,......,N. \qquad ......(10\text{-}12)$$

Noting that β_0 and γ appeared in above relations can be expressed in terms of the area reduction parameter r and the "artificial semi-angle" of the die α respectively as:

$$\beta_0 = \sqrt{1-r} \quad , \quad \gamma = \frac{1-\beta_0}{\tan\alpha} \qquad ......(13\text{-}14)$$

The present expression of the die internal pressure P_r, in eq.(11), may be evaluated successfully starting by $i=1$, where $(\sigma_x/\sigma_Y=0)$ and making $\phi_0=\phi_1$ as a unique approximation in this stage. The system of eqs.(10-11) gives evidently a "*best*" result as long as the integer N goes larger enough.

Typical Die Profile Curves:

The billet-die stresses P_r and σ_x depend very strongly on the ratio β as being indicated by eqs.(10-11), or specifically on the type of $R=f(x)$. In order to verify the use of these expressions, two typical profiles of the die surface were chosen. The first one is the familiar "*truncated*" conical type in which:

$$\tan\alpha_i = \phi_i = \text{cons}\tan t \qquad ......(15)$$

everywhere. Applying this condition on the total interval $(x_N\text{-}x_0)$ and any other interval $(x_i\text{-}x_0)$ will yield:

$$\frac{R_i - R_0}{(iL/N)} = \frac{R_N - R_0}{L} \quad \text{from which}$$

$$\beta_i = \beta_0 + \frac{i(1-\beta_0)}{N} \qquad i = 0,1,2,....,N \qquad ......(16)$$

The second die profile is the "*radial convex*" one, where the inner curved line is a portion of circumference of radius r_0 whose center is upward the die exit location. At this position, the curve radius satisfies the identity of:

$$r_0^2 = L^2 + \left(r_0 - (R_N - R_0)\right)^2 \quad \text{from which :}$$

$$\left(\frac{r_0}{R_N}\right) = \frac{\gamma^2 + (1-\beta_0)^2}{2(1-\beta_0)} \qquad ......(17)$$

whereas at any arbitrary location:

$$r_0^2 = L^2 + \left(x_i - (R_N - R_0)\right)^2 \quad \text{which implies inturn :}$$

$$\beta_i = \beta_0 + \left(\frac{r_0}{R_N}\right) - \sqrt{\left(\frac{r_0}{R_N}\right)^2 - \left(\frac{i\gamma}{N}\right)^2} \qquad i = 0,1,2,.....,N \qquad ......(18)$$

and by this, the two typical profiles will be ready to execute the present traction eqs.(10-12).

Numerical results and discussion:

First of all, a check of convergence pattern of the numerical results, from eqs.(10-11), should be taken over, since the proper level of the final results depends widely upon the selected value of the offset's number *N*. The convergence of $(\sigma_x/\sigma_Y)_{max}$, from eq.(10), can be sufficient for this investigation, while (P_r/σ_Y), in eq.(11), is related directly to the former item. Table(1) shows the theoretical estimations of (σ_x/σ_Y) for two conditions of the billet area reduction *r*, each for two selected values of the die semi-angle α. The die internal profile is chosen to be the "*radial convex*", as explained before with $m=0.065$, whereas the convergence of results is tested for five values of $N=1,10,50,100$ and *200.* As can be noticed, all numeric are quit converging to the stable values for $N=100$ and more precisely for $N=200$. The running time of the applied software, for this purpose, is found extremely short (less

Table(1) Convergence pattern of *(σ_x/σ_Y)* in "*radial convex*" die for five offset's number , two reduction areas and artificial semi-angle, in accordance to SSM.

Offset number	r=30%		r=70%	
	α=25degs.	α=65degs.	α=25degs.	α=65degs.
1	**2.34**	**2.34**	**2.93**	**1.59**
10	**3.41**	**2.37**	**3.66**	**1.85**
50	**3.57**	**2.49**	**3.75**	**1.89**
100	**3.59**	**2.50**	**3.76**	**1.90**
200	**3.60**	**2.51**	**3.76**	**1.90**

Table(2). The traction ratio *(P_r/σ_Y)* of two typical die profiles for several choices of friction factor, artificial semi-angle, area reduction and at different positions along the central axis.

x/L	m	**Truncated Conical Die**				***Radial Convex Die***			
		α=15degs.		α=55degs.		α=15degs.		α=55degs.	
		r=20%	r=60%	r=20%	r=60%	r=20%	r=60%	r=20%	r=60%
1.00	**0.00**	**1.9292**	**2.3065**	**4.9861**	**3.9962**	**2.5889**	**2.6247**	**5.4091**	**3.0978**
	0.03	**1.9493**	**2.3746**	**5.0191**	**4.0547**	**2.6145**	**2.7041**	**5.4510**	**3.1576**
	0.06	**1.9694**	**2.4428**	**5.0520**	**4.1132**	**2.6410**	**2.7836**	**5.4928**	**3.2174**
	0.09	**1.9895**	**2.5109**	**5.0850**	**4.1717**	**2.6656**	**2.8630**	**5.5346**	**3.2773**
	0.12	**2.0096**	**2.5790**	**5.1180**	**4.2302**	**2.6912**	**2.9424**	**5.5765**	**3.3371**
	0.15	**2.0297**	**2.6471**	**5.1509**	**4.2887**	**2.7168**	**3.0218**	**5.6183**	**3.3969**
0.75	**0.00**	**1.8064**	**2.0319**	**4.5633**	**3.3673**	**1.9205**	**1.8668**	**2.6707**	**1.7010**
	0.03	**1.8228**	**2.0867**	**4.5943**	**3.4187**	**1.9389**	**1.9272**	**2.6888**	**1.7290**
	0.06	**1.8392**	**2.1415**	**4.6253**	**3.4701**	**1.9572**	**1.9875**	**2.7069**	**1.7571**
	0.09	**1.8556**	**2.1962**	**4.6563**	**3.5215**	**1.9755**	**2.0479**	**2.7251**	**1.7851**
	0.12	**1.8720**	**2.2510**	**4.6873**	**3.5729**	**1.9939**	**2.1083**	**2.7432**	**1.8132**
	0.15	**1.8883**	**2.3058**	**4.7183**	**3.6244**	**2.0122**	**2.1686**	**2.7613**	**1.8412**
0.50	**0.00**	**1.6834**	**1.7404**	**4.1460**	**2.7374**	**1.4873**	**1.3861**	**1.8351**	**1.2934**
	0.03	**1.6960**	**1.7804**	**4.1749**	**2.7809**	**1.4991**	**1.4268**	**1.8450**	**1.3092**
	0.06	**1.7086**	**1.8204**	**4.2039**	**2.8244**	**1.5109**	**1.4676**	**1.5848**	**1.3250**
	0.09	**1.7212**	**1.8604**	**4.2328**	**2.8680**	**1.5227**	**1.5084**	**1.8646**	**1.3408**
	0.12	**1.7338**	**1.9004**	**4.2618**	**2.9115**	**1.5345**	**1.5492**	**1.8744**	**1.3566**
	0.15	**1.7463**	**1.9403**	**4.2908**	**2.9551**	**1.5463**	**1.5900**	**1.8843**	**1.3724**
0.25	**0.00**	**1.5602**	**1.4279**	**3.7342**	**2.1060**	**1.1900**	**1.1071**	**1.3343**	**1.0939**
	0.03	**1.5689**	**1.4514**	**3.7611**	**2.1408**	**1.1956**	**1.1275**	**1.3385**	**1.1010**
	0.06	**1.5776**	**1.4748**	**3.7880**	**2.1755**	**1.2012**	**1.1480**	**1.3427**	**1.1080**
	0.09	**1.5863**	**1.4982**	**3.8149**	**2.2102**	**1.2069**	**1.1685**	**1.3469**	**1.1150**
	0.12	**1.5949**	**1.5217**	**3.8418**	**2.2450**	**1.2125**	**1.1889**	**1.3511**	**1.1221**
	0.15	**1.6036**	**1.5451**	**3.8686**	**2.2797**	**1.2182**	**1.2094**	**1.3553**	**1.1291**
0.00	**0.00**	**1.0639**	**1.0130**	**1.0639**	**1.0130**	**1.0639**	**1.0130**	**1.0639**	**1.0130**

	0.03	**1.0646**	**1.0137**	**1.0696**	**1.0137**	**1.0646**	**1.0137**	**1.0646**	**1.0137**
	0.06	**1.0653**	**1.0143**	**1.0653**	**1.0143**	**1.0653**	**1.0143**	**1.0653**	**1.0143**
	0.09	**1.0660**	**1.0150**	**1.0660**	**1.0150**	**1.0660**	**1.0150**	**1.0660**	**1.0150**
	0.12	**1.0667**	**1.0157**	**1.0667**	**1.0157**	**1.0667**	**1.0157**	**1.0667**	**1.0157**
	0.15	**1.0673**	**1.0164**	**1.0673**	**1.0164**	**1.0673**	**1.0164**	**1.0673**	**1.0164**

than 3 seconds). Figs.(2,3) illustrates the variation of (P_r/σ_Y) magnitude with the probable values of r. Six different situations of α value were adopted, but for fixed friction factor *(m=0.05)*. The single curved line of (P_r/σ_Y), in each figure, is corresponding to one particular position within the die region, i.e for one assignment of *(x/L)*, out from the set *(0, 0.1, 0.2, ….,1.0)*. In these eleven curves, the ratio *(x/L=0)* belongs to the die entrance position, and *(x/L=1)* refers to the die exit position. Fig.(2) relates with the "*truncated conical*" shape of the die, while Fig.(3) for the "*radial convex*" one. A little consideration into these plotting, gives a conclusion of that the conical die shows no much variation of pressure with *(x/L)* at small reduction of area $(r \leq 0.15)$, in the contrary with the "*radial convex*" die, moreover there exits a trend of increasing with r for small angle values $(\alpha \leq 5$ *degrees)*, in opposite to that for larger angles (as shown for $\alpha=80$ degrees) and for the two die shapes equally. However, the "*radial convex*" die gives almost linear and uniform variation of (P_r/σ_Y) with r, near the die exit region $(x/L \leq 0.1)$. Finally an investigation into the role of the friction factor m upon (P_r/σ_Y) was made as shown by Table(2), where the two die profiles were adopted, each for two selected values for both α and r independently. The table is subdivided into five main rows for *(x/L=1, ¾, ½, ¼ and 0)*, each row covers six selected values of *(m=0, 0.03, 0.06,…,0.15)*. As can be seen, the pressure ratio increases naturally with m, for all conditions of the input data, however, no much increase is noticed at the die exit position *(x/L=0)*. Nevertheless, for fixed *(x/L)* value, the two die profiles, with small artificial angle ($\alpha=15$ degrees), show an increase with r, but for ($\alpha=55$ degrees) they show a decreasing trend. In spite of that, the "*radial convex*" die gives the results less in values than the corresponding ones of the "*truncated conical*" die, for larger magnitudes of the artificial semi-angle. Table(3) confirms the thought that the present SSM *over-estimates* the inlet pressure ratio compared to that of the CSM for all manufactured truncated-dies adapted from Refs. [11,12]. As soon as the internal traction, at the die internal surface, is completely estimated, The engineering design, correcting and control would be guaranteed for the next stage of point-wise stress and strain analyzing with the help of applied packages of the finite-element methods as usual.

Conclusions:

As a closing remark, One can shad a light on three main things out of previous theoretical-numerical treatment and as followings:

(a) A new advanced formula of the die internal surface pressure (eq.(12)) is found now very useful to compute the local die pressure at any point within the surface. The new SSM [13] predicts accurate results of the pressure upon the CSM for the allowance of the transverse shear stress included in.

(b) The proposed numerical procedure to evaluate the die internal surface pressure, by combining of the SSM with FI approach, seems very active tool to deal with such problem with good converging results depending on the selected numbers of the axis subdivisions.

(c) The present procedure can be reliably applied regardingless the formatic shape of the die internal surface. The chosen two industrial types of the die had been analyzed successfully to estimate the related pressure values in point-wise manner.

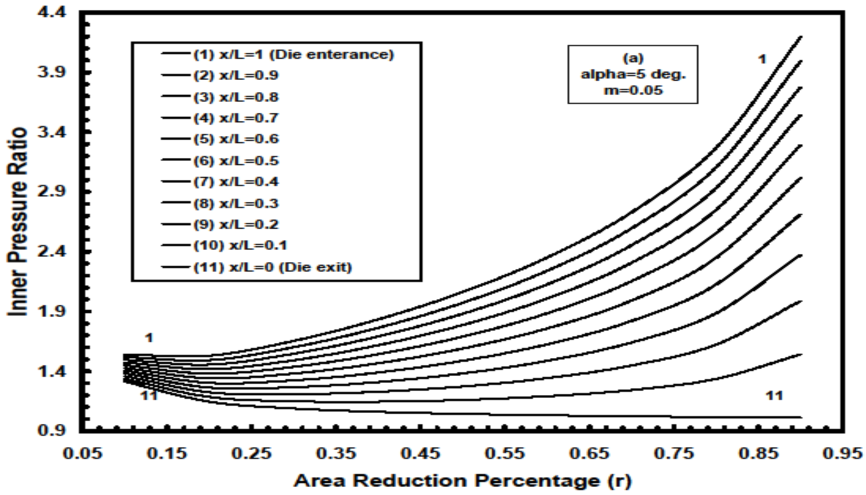

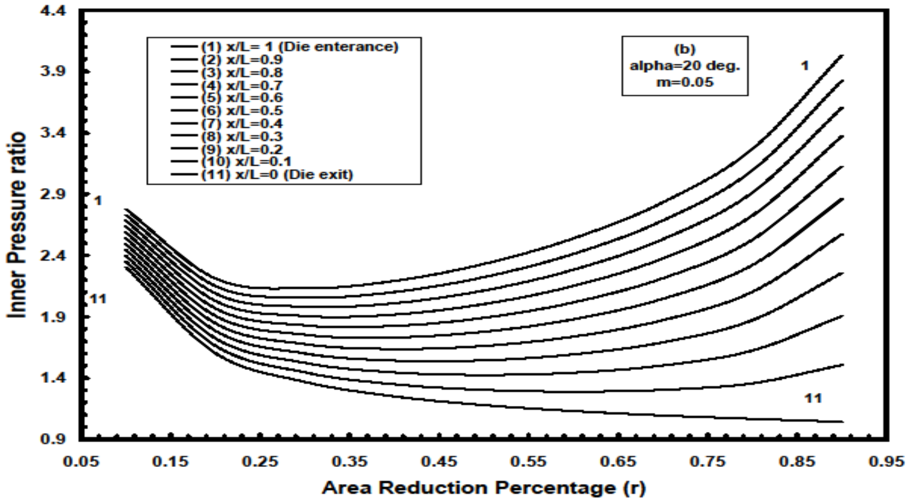

Figs. (2a, 2b) Variation Of (P_r/σ_Y) With ® Along "*Conical*" Die For Fixed Friction Factor And Two Different Die Semi-Angles.

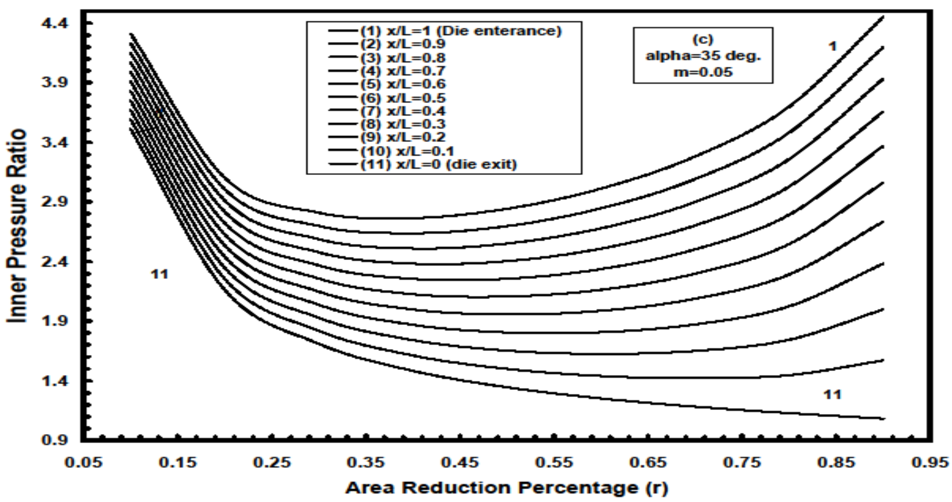

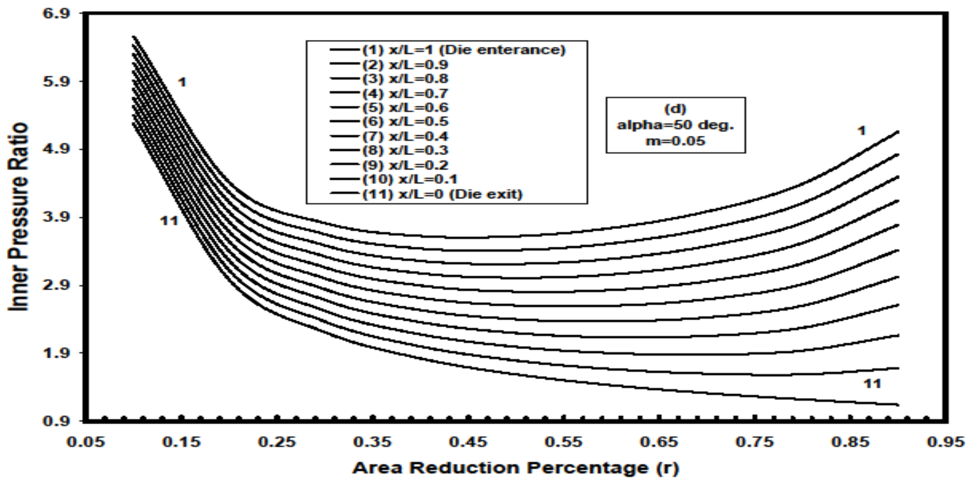

Figs. (2c, 2d) Variation Of (P_r/σ_Y) With ® Along "*Conical*" Die For Fixed Friction Factor And Two Different Die Semi-Angles.

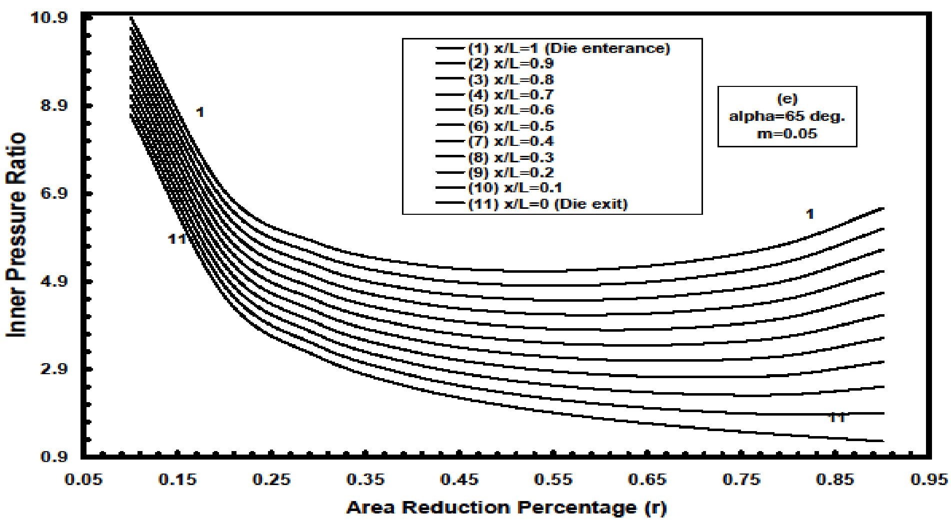

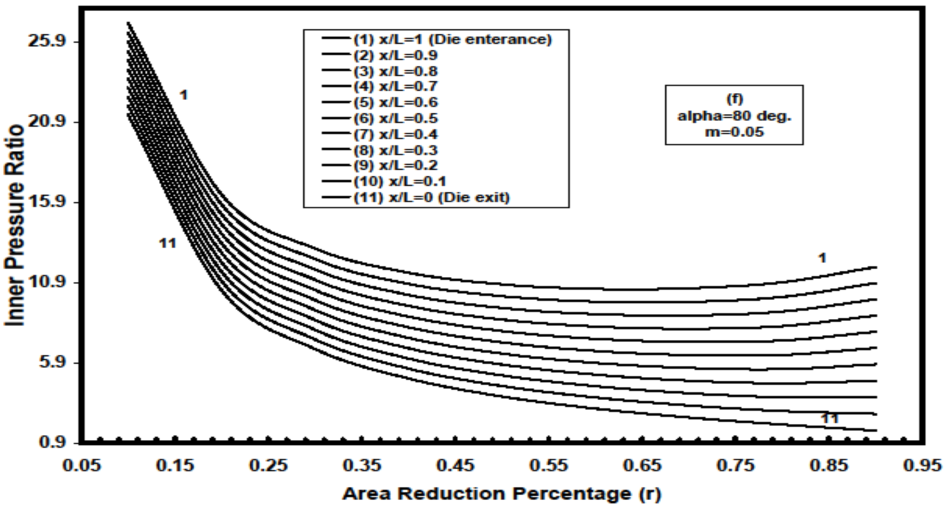

Figs. (2e, 2f) Variation Of (P_r/σ_Y) With ® Along "*Conical*" Die For Fixed Friction Factor And Two Different Die Semi-Angles.

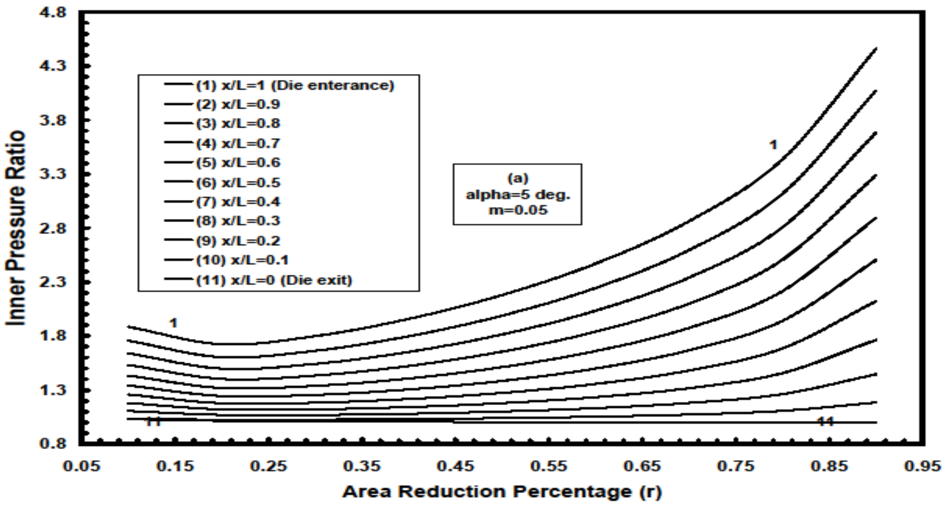

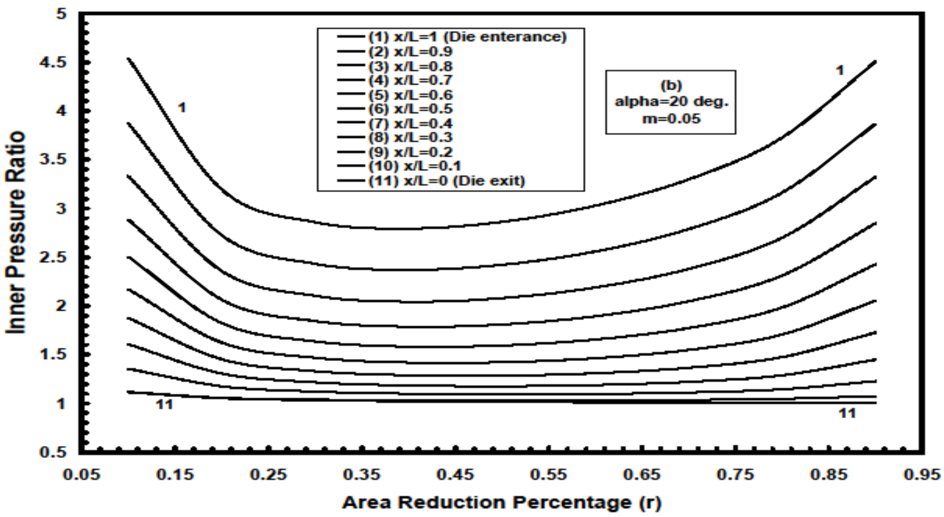

Figs. (3a, 3b) Variation Of (P_r/σ_Y) With ® Along "*Radial*" Die For Fixed Friction Factor And Two Different Die Semi-Angles.

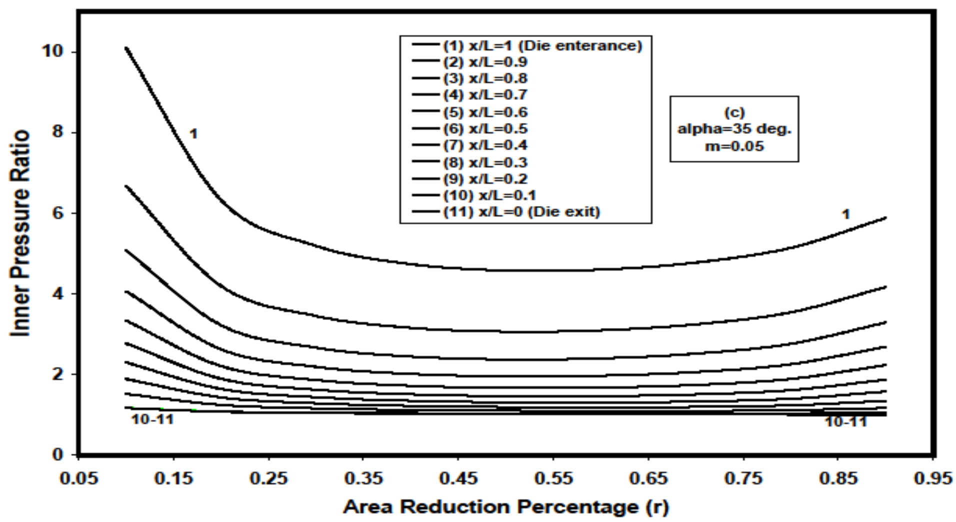

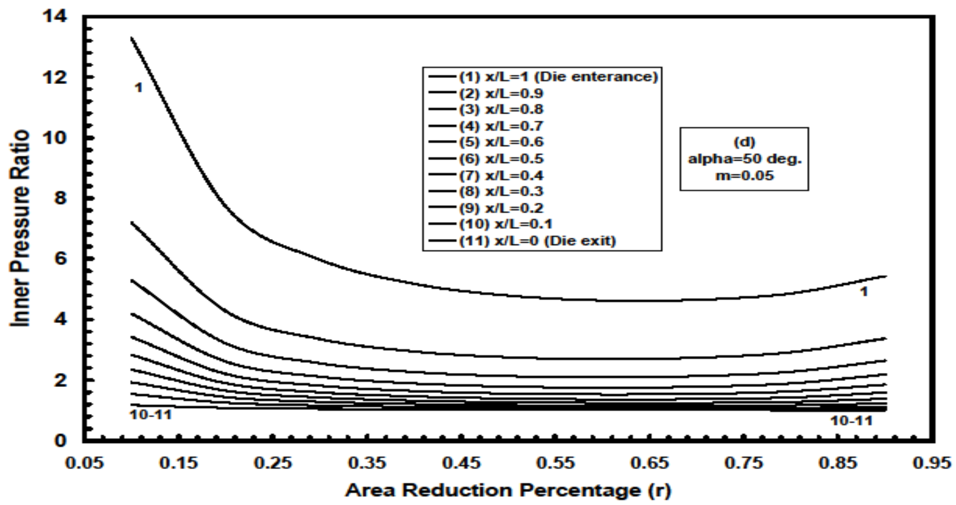

Figs. (3c, 3d) Variation Of (P_r/σ_Y) With (r) Along "*Radial*" Die For Fixed Friction Factor And Two Different Die Semi-Angles.

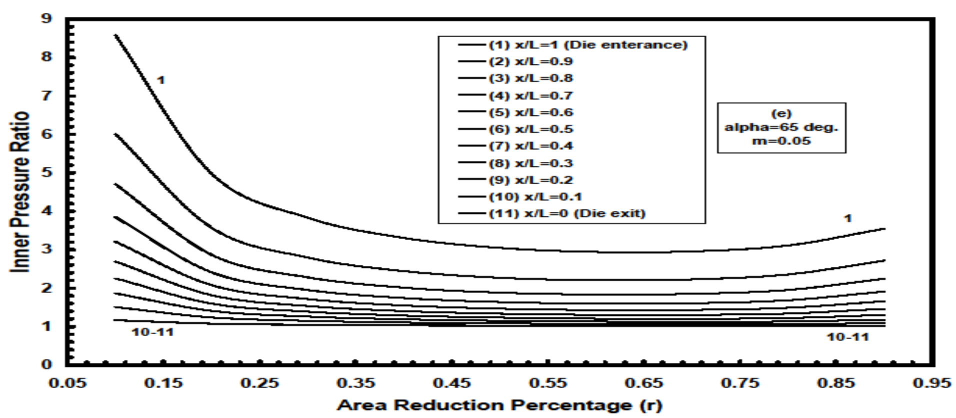

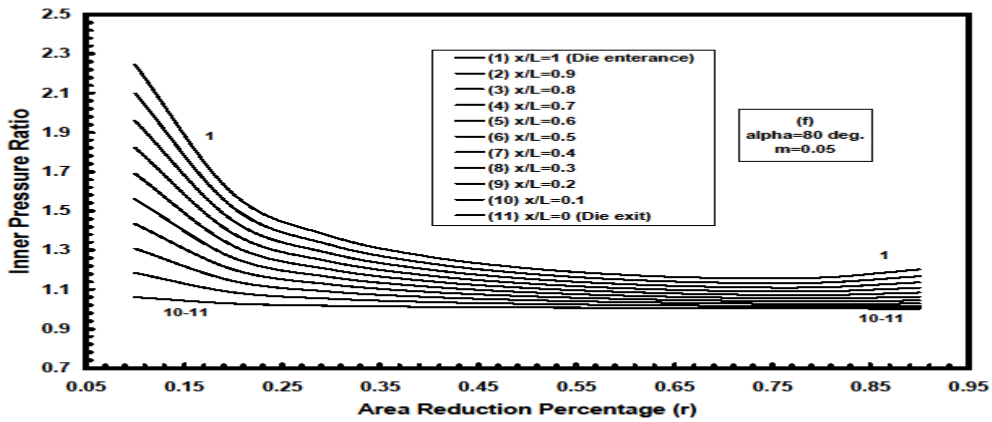

Figs. (3e, 3f) Variation Of (P_r/σ_Y) With (r) Along "*Radial*" Die For Fixed Friction Factor And Two Different Die Semi-Angles.

Table(3) Comparison of the die inlet pressure ratio (P_r/σ_Y) for typical "*truncated conical*" die of r=30% and m=0.044 .

Die semi-angle α (deg.)	Experimental (σ_x/σ_Y) [11,12]	(P_r/σ_Y)	
		CSM [5,13]	***Present SSM***
2.33	**0.56**	**1.5806**	**1.6626**
3.33	**0.52**	**1.5138**	**1.6314**
5.00	**0.50**	**1.4622**	**1.6400**
6.50	**0.475**	**1.4389**	**1.6700**
8.00	**0.485**	**1.4275**	**1.7093**
10.00	**0.50**	**1.4125**	**1.7692**
11.50	**0.52**	**1.4062**	**1.8182**

References:

1. Li L, Rao K., Lou Y. and Peng D., "A study On Hot Extrusion Of Ti-6Al-4V Using Simulations And Experiments", *Int. J. Mech. Sci.,* 2002, Vol. 44, pp. 2415-2425.
2. Lof J., *Development In Finite Element Simulations Of Aluminum Extrusion,* Ph.D Thesis, University of Twente, The Netherlands, 2000.
3. Avitzur B., "Metal Forming: Processes And Analysis*", Mc-Graw Hill series in materials science and engineering*, New York, 1968.
4. Suchs G., Lubahn J. and Tracy D., "Drawing Of Thin-Walled Tubing", *J. Appl. Mech.,* 1944, Vol. 11, pp. 199-210.
5. Avitzur B., "Flow characteristics Through Conical Converging Dies", *J. Engg. Ind., Trans. ASME*, series B, 1966, Vol. 88, pp. 410-420.
6. Yang D., Lee C. and Yoon J., "Finite Element Analysis Of Steady-State Three Dimension Extrusion Of Section Through Curved Dies", *Int. J. Mech. Sci.,* 1989, Vol. 31, pp. 145-

156.

7. Udagawa T., Kroop E. and Altan T., "Investigation Of Metal Flow And Temperature By FEM In The Extrusion Of Ti-6Al-4V Tubes", *J. Mat. Proces. Tech.,* 1992, Vol. 33, pp. 155-174.

8. Johnson W. and Moller D*., Engineering Plasticity,* Ellis Horwood Limited, England, 1986.

9. Ford H. and Finner R., "Elasticity and Plasticity In Engineering.", *Imperial College Of Sciences And Technology,* England, 1989.

10. Green D., "Continuous Extrusion-Forming Of Wire Sections", *J. Inst. Metals*, 1972, Vol. 100, pp. 295-300.

11. Avitzur B., "Limit Analysis Of Flow Through Conical Converging Dies", *The Winter Annual Meeting Of The ASME*, 1981, Nov. 15-20, pp. 167-197.

12. Wistreich J.," Investigation Of The Mechanics Of Wire Drawing", *Proc. Inst. Mech. Engr. (London),* 1955, Vol. 169, pp. 654-665.

13. Saify K.M., "The Sheared-Slab Method (SSM): A Modification On The Classical Slab Method (CSM) For Extrusion Analysis Through Conical Dies", ought to be appeared at *AL-Tachani J.*, FTE, 2005.

14. Iiers F., *Theories And Problems In Calculus For Engineers*, Mc-Graw Hill, England, 1976.